AIAA JOURNAL
Vol. 30, No. 5, May 1992

Exploratory Design Studies of Actively Controlled Wings Using Integrated Multidisciplinary Synthesis

E. Livine,* L. A. Schmit,† and P. P. Friedmann‡
University of California, Los Angeles, Los Angeles, California 90024

Analysis and synthesis techniques used in a newly developed, multidisciplinary, control augmented, structural wing optimization capability are reviewed. Structural, aerodynamic, and control system mathematical models that are suitable for the preliminary design of real airplanes are used in an integrated manner to synthesize improved designs of wings and their active control systems. Optimization techniques developed for structural synthesis are adapted to the integrated multidisciplinary wing synthesis problem, in which constraints from several disciplines are taken into account simultaneously and the design space is opened up to include structural and control system design variables. The effectiveness and efficiency of the new capability are studied using a mathematical model of a remotely piloted vehicle.

Nomenclature

$[\tilde{A}], [\tilde{B}]$ = state-space system matrices of the aeroservoelastic system in standard form
A_0, A_1 = spar and rib cross-sectional area structural design variables [Eq. (4)]
a_c, b_c, c_c = control system design variables [Eq. (13)]
$\{C_k\}$ = transformation vector relating the system's state vector to system output k
$F(\{X\})$ = objective function
$g(\{X\})$ = vector of inequality constraints
H_i = coefficients of the polynomial series for wing depth [Eq. (2)]
$h(x,y)$ = wing depth
$[K]$ = structural stiffness matrix
$[\tilde{K}]$ = aeroelastic stiffness matrix
$\{\tilde{P}\}$ = vector of generalized loads in maneuver (dependent on structural design variables)
$[Q_w]$ = intensity matrix of the Gaussian white noise
$\{q\}$ = vector of generalized structural displacements
$\{\tilde{q}\}$ = vector of generalized structural displacements and control surface rotations at a given maneuver point
q_c = control surface rotation
s = Laplace variable
T_i = coefficients of the polynomial series for wing skin thickness distribution [Eq. (3)]
$t(x,y)$ = wing skin thickness distribution
$[U], [V], [W]$ = aeroservoelastic system state-space model matrices [Eq. (6)]
$\{\hat{w}\}$ = zero mean Gaussian white noise
$\ddot{w}_{0.65c}$ = actual vertical acceleration at the accelerometer location at 0.65 chord on the wing strip containing the aileron
$[X]$ = state covariance matrix
$\{X\}$ = vector of design variables
$\{X\}^L$ = vector of design variables' lower bounds
$\{X\}^U$ = vector of design variables' upper bounds
$\{x(s)\}$ = Laplace transformed state vector of the aeroservoelastic system
y_k = system output k
y_{SE} = sensor output
δ = actuator command = control law output
η = coordinate along spar or rib length
ω_c = equivalent natural frequency of the control law transfer function (second order)
ζ_c = equivalent viscous damping of the control law transfer function (second order)

Introduction

MULTIDISCIPLINARY interactions have always been central in airplane wing design. The introduction of active control technology[1-3] and composite structural tailoring[4-6] during the last 15 years have made these interactions more complex and important. Experience has shown that incomplete treatment of multidisciplinary interactions during the design process can lead to dangerous consequences.[7,8] At the same time, the benefits of multidisciplinary integration have become widely recognized motivating extensive research and influencing design.[9-11] Still the design practice of the past, which was based on a sequential, compartmented approach, is often followed today. True, advanced analysis and testing tools have been developed to address multidisciplinary interactions. Active flutter suppression, maneuver load control, gust alleviation, and ride smoothing techniques are utilized, to mention a few examples. Optimization techniques are used for control system synthesis, aerodynamic design, and aeroelastic tailoring. Structural wing synthesis subject to structural, aeroelastic, and aerodynamic performance constraints has successfully followed in the footsteps of structural synthesis[12,13] using a variety of computer codes and techniques.[14-18] However, the application of optimization techniques to multidisciplinary wing design is still in its infancy. True integration in design involving structures, aerodynamics, and performance simultaneously is described in Refs. 19 and 20. The synthesis of realistic wings subject to a set of multidisciplinary constraints addressing design variables influencing several disciplines including controls has not been carried out. This integrated synthesis of a wing structure and its active control system is particularly complex and difficult. In the few cases where it was studied,[21-23] the mathematical models used were

Presented as Paper 90-0953 at the AIAA/ASME/ASCE/AHS/ASC 31st Structures, Structural Dynamics, and Materials Conference, Long Beach, CA, April 2-4, 1990; received Oct. 23, 1990; revision received June 14, 1991; accepted for publication June 18, 1991.

*Assistant Research Engineer, Mechanical, Aerospace and Nuclear Engineering Department; currently, Assistant Professor, Aeronautics and Astronautics, Univ. of Washington, Seattle, WA.

†Rockwell Professor of Aerospace Engineering, Emeritus, Mechanical, Aerospace and Nuclear Engineering Department.

‡Professor, Mechanical, Aerospace and Nuclear Engineering Department.

so simplified that they did not provide an assessment of the techniques needed to optimize realistic wings, and the accumulation of practical design experience was not possible. Thus, the application of modern optimization techniques to wing design involving a diverse mix of constraints and design variables based on analyses from several disciplines (structures, structural dynamics, aeroelasticity, control, and handling qualities) has not yet been treated in a comprehensive and realistic manner.

Reference 24 describes a synthesis capability for actively controlled fiber composite lifting surfaces. It discusses structural, aerodynamic, and control system modeling techniques adopted and modified to challenge the formidable computational task of carrying out analysis and behavior sensitivity calculations for this problem with computer resources that make optimization practical and with accuracy that is sufficient for preliminary design. It is based on the generalization of the nonlinear programming/approximation concepts (NLP/AC)[12,13] approach from structural synthesis to multidisciplinary optimization. The present paper focuses on the control augmented, aeroservoelastic, structural synthesis problem and reports results achieved using the new capability.[24] The applicability of approximation concepts to the control augmented, structural synthesis of wings is studied. Examination of optimization convergence as influenced by including approximations of new constraints (particularly aeroservoelastic stability and gust-response constraints) guides identification of effective move limits, convergence criteria, and approximation types to be used. Examples of integrated optimization of a realistic wing and its active control system with structural and control system design variables subject to gauge, stress, aeroservoelastic stability, and gust-response constraints offer an improved understanding of this complex synthesis problem.

Review of Mathematical Modeling Techniques

The integrated optimum design capability is based on a unique integration of analysis techniques for the required disciplines. Their selection is a tradeoff between accuracy and detail and the computational resources required.[24] In the structures area, a rather general equivalent plate analysis[25] which builds on the basic ideas underlying the TSO computer code[14] and incorporates additional recent developments proposed by Giles[26] is used. Configurations made of several plate segments can be analyzed to simulate wing/control surface configurations. The equivalent plate structural analysis documented in Ref. 25 is integrated with the piecewise continuous kernel function method (PCKFM) developed by Nissim and Lottati for lifting surface unsteady aerodynamics.[27-30] This method is particularly suitable for calculating the generalized unsteady air loads (on lifting surfaces made up of wing and control surface elements) that are needed for active flutter suppression and gust-alleviation studies. When the optimization of the design for aeroservoelastic stability is addressed and modern control techniques are to be implemented, it is necessary to cast the aeroelastic equations of motion in linear time invariant (LTI) state-space form. It then follows that some approximation of the unsteady aerodynamic loads in terms of rational functions of the Laplace variable is needed. The method of Roger[31] has been widely used for finite-dimensional unsteady aerodynamic loads representation for quite a while. The minimum state method, developed by Karpel[32] and studied in Ref. 33, is found to be attractive because it has the potential for generating accurate approximations to unsteady generalized aerodynamic forces, while adding only a small number of augmented states to the mathematical model of the aeroservoelastic system. Both methods are available in the present capability. The integrated aeroservoelastic system is modeled as an LTI system. Since the number of sensors and control surfaces is small in real airplanes, complex, high-order control laws generated by some modern multi-input multi-output (MIMO) control system design techniques are avoided at this stage. A block diagram of the actively controlled aeroservoelastic system is shown in Fig. 1. Airplane motions (acceleration and angular rates) are measured by a set of sensors placed on the structure. The resulting signals y_{SE} are used as inputs to the control law block which commands control surface actuators. The control surface motions q_c guarantee stability and desirable dynamic response of the complete system. The control system is completely described by the location of sensors and control surfaces and by the transfer functions of the sensors, control laws and actuators. Gain scheduling can be adopted by assigning different control laws to different flight conditions.

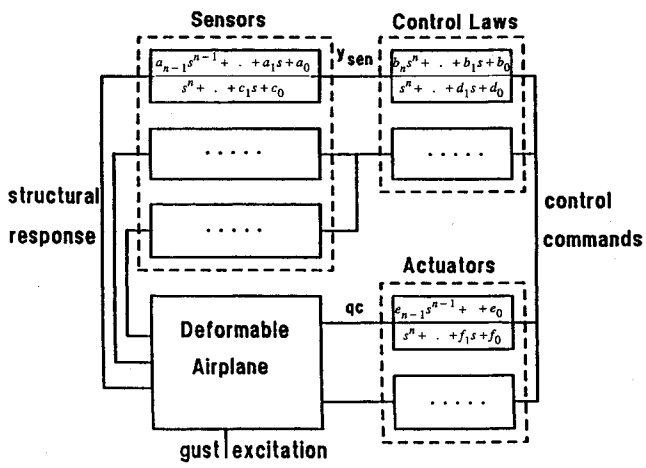

Fig. 1 Aeroservoelastic control system modeling.

The combination of modern equivalent plate structural modeling, PCKFM lifting surface aerodynamics, and LTI MIMO control system modeling is assumed to be adequate for this exploratory venture into multidisciplinary practical wing synthesis. In addition to a reliable prediction of deformations, stresses, flutter results, and static aeroelastic effects, quite good hinge moments[34] and induced drag[35,36] can be expected for subsonic and supersonic small angle-of-attack flight. The analysis is adequate for addressing flight stability and control problems of the elastic airplane.[37] Its aerodynamic predictions might be improved by using correction-factor techniques if any measured data are available. As to control system modeling, the techniques used here make it possible to properly model real flight control or active flutter suppression systems. Effects of real actuators and sensors on control system performance are automatically taken into account through their given transfer functions.

Design Variables

Reference 24 sets forth a framework for multidisciplinary wing synthesis and describes a hierarchy of design variables consisting of sizing type design variables at the lowest level, followed by shape and then topological type design variables. This classification applies to design variables spanning structures, control, and aerodynamics. The higher the location of design variables in this hierarchy in a particular design synthesis problem, the more complex and computationally intensive is the synthesis. In the present study of combined structure/control aeroservoelastric synthesis, a balance is maintained in level of optimization complexity by focusing on sizing type design variables for all disciplines considered.

Structural Design Variables

Figure 2 shows an airplane modeled as an assembly of flexible lifting surfaces. Each lifting surface is modeled as an equivalent plate whose stiffness is controlled by contributions from thin cover skins (fiber composite laminates) and the internal structure (spar and rib caps). Plate sections are connected to each other via stiff springs (representing hinge stiffness at attachment points) and flexible springs (representing the stiffness of actuators and their backup structure). Each

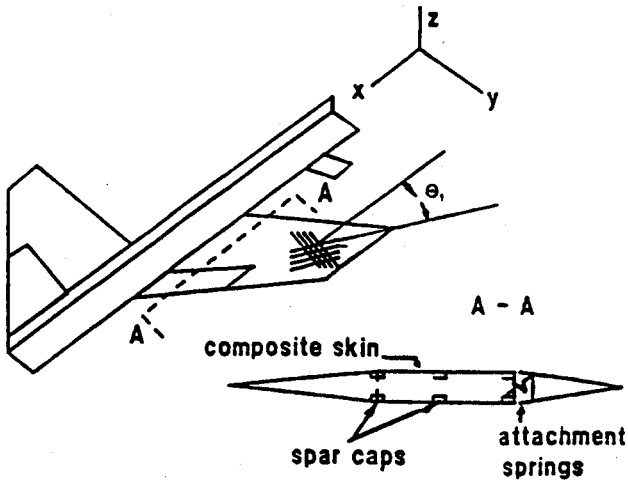

Fig. 2 Equivalent plate structural modeling.

wing section can be represented as a combination of several trapezoidal segments. Concentrated masses are used to model nonstructural items and balance masses. The vertical displacement w of each section is approximated by a Ritz polynomial series of the form

$$w(x,y,t) = \sum_{i=1}^{Nw} q_i\langle t\rangle x^{mi} y^{ni} \tag{1}$$

where x and y are chordwise and spanwise coordinates, respectively, and mi and ni are powers describing the type of polynomial series used. It can be a complete polynomial in x and y or a product of polynomials in x and y (Ref. 25). The depth of a wing section is given by a polynomial

$$h(x,y) = \sum_{i=1}^{Nh} H_i x^{ri} y^{si} \tag{2}$$

where the H_i are preassigned parameters. Thickness distribution of a typical skin layer is represented by

$$t(x,y) = \sum_{i=1}^{Nt} T_i x^{ki} y^{li} \tag{3}$$

Rib and spar cap areas are allowed to vary linearly over their length η

$$A(\eta) = A_0 + A_1\eta \tag{4}$$

The present equivalent plate modeling capability[25] makes it possible to efficiently analyze combined wing box/control surface configurations. At the present stage of research structural topology, planform shape, airfoil shape, and material properties are preassigned. Only sizing type design variables are used. For skin-layer thicknesses [Eq. (3)], the coefficients of the thickness power series serve as design variables. This guarantees smooth thickness variation for each layer. For spar and rib cap areas [Eq. (4)], two coefficients are used as design variables for each spar or rib. Concentrated masses at preassigned locations and spring constants for linear and rotational springs can also be treated as design variables.

Control System Design Variables

The control system design variables are limited at this stage of research to sizing variables, namely the values of coefficients in the numerator and denominator of control law transfer functions (Fig. 1). Other parametrizations of the controller exist, of course, and controllers for the current aeroservoelastic models could be synthesized using more advanced MIMO control system design techniques. The direct transfer function synthesis approach adopted here makes it possible to treat quite complex and realistic control systems as well as very simple controllers. It is in balance with the sizing level treatment of the structural synthesis. Furthermore, it is general enough to allow study of realistic interplay between structure and controls in integrated aeroservoelastic synthesis. Thus, control surface locations, sensor locations, topology of the control system, and the order of numerator and denominator polynomials in the transfer functions are preassigned. It is assumed here that sensor and actuator transfer function are preassigned, although the formulation allows the treatment of their numerator and denominator coefficients as additional design variables.

The set of design variables treated here spans two disciplines, namely structures and control. The design space is thus opened up to simultaneously span sizing level design variables from these two disciplines.

Analysis Capabilities

To provide a rich variety of constraints and alternative objective functions, the following analysis capabilities are included.

Static "Maneuver Load" Analysis

Static aeroelastic deflections and stresses are calculated for the elastic airplane in maneuver. Maneuvers include symmetric pull ups (defined by Mach number, altitude, and load factor) or steady rolling maneuvers (defined by Mach number, altitude, and roll rate). In addition to elastic deflections and stresses, the control surface deflections and hinge moments needed for the maneuvers are obtained. Maneuver deflection and stress analysis consists of solving the equations of motion of the free-free deformable airplane in maneuver. In a stiffness formulation based on the Ritz polynomial functions used in Eq. (1), these equations take the form

$$[\tilde{K}]\{\tilde{q}\} = \{\tilde{P}\} \tag{5}$$

where $\{\tilde{q}\}$ is a vector of generalized displacements including an added control surface rotation degree of freedom needed for trim in pull-up or in roll. The matrix $[\tilde{K}]$ is a nonsymmetric matrix whose elements are combinations of structural stiffness, aerodynamic stiffness, and aerodynamic control surface stiffness terms. The vector $\{\tilde{P}\}$ depends on inertial forces, jig shape (initial undeformed shape of the wing), and deflection setting of additional control surfaces for drag or load modification.

Aeroservoelastic Stability Analysis

Poles of the LTI state-space model of the control augmented airplane are calculated for different flight conditions and boundary conditions (cantilevered, symmetric or antisymmetric free-free motion). Assembly of the state-space models of the structure, sensors, actuators, control laws, as well as approximate unsteady air load and gust aerodynamics, leads to the closed-loop state-space equations of the complete system in the form

$$s[U]\{x(s)\} = [V]\{x(s)\} + \{W\}\hat{w} \tag{6}$$

A "gust filter" is used to transform a zero mean Gaussian white noise input $\hat{w}$ into a vertical gust speed of given power spectral density and root mean square (rms) value which represents the structural excitation due to atmospheric turbulence. The state vector $\{x\}$ contains structural, sensor, actuator, control law, gust filter, and aerodynamic states. The system matrices $[U]$ and $[V]$ depend on structural and control system design variables.[24] Full-order structural modeling is possible when all Ritz polynomials of Eq. (1) are used for stiffness, mass, and aerodynamic terms of U, V, and W. This, however, is extremely expensive computationally even for the relatively small number of polynomials needed for structural modeling

of a typical configuration (20 − 80) and it was used only for order-reduction convergence studies. Otherwise, modal truncation order-reduction methods are used based on either a subset of natural modes of the current design calculated with each approximate problem generation[38] or a set of "mass modified" fixed modes[39,40] periodically updated after a preassigned number of full analyses (e.g., three). Finite-dimensional state-space unsteady aerodynamic approximations can be generated for the full-order aerodynamic matrices at the start of optimization, or directly for modally reduced aerodynamic matrices during optimization whenever the modal basis is changed.[24]

Gust Response Analysis

The rms values of control surface deflections and rates as well as rms values of selected sensor measurements due to continuous atmospheric turbulence are calculated for different flight conditions. Both Dryden and rational approximations for the von Kármán turbulence spectra are implemented. The relevant quantities are rms values of control surface deflections $\{q_c\}$, rates $\{\dot{q}_c\}$, and sensor measurements $\{y_{SE}\}$. The state space equations [Eq. (6)] are transformed into standard form

$$s\{x(s)\} = [\tilde{A}]\{x(s)\} + \{\tilde{B}\}\hat{w}(s) \tag{7}$$

Since only $\{q_c\}$, $s\{q_c\}$, and $\{y_{SE}\}$ are considered,[24] a typical output y_k is given by

$$y_k = \{C_k\}^T\{x\} \tag{8}$$

where $\{C_k\}$ is either constant or a function of control system design variables. The state covariance matrix is a solution of a Lyapunov's matrix equation[41] in the form

$$[\tilde{A}][X] + [X][\tilde{A}]^T = -\{\tilde{B}\}[Q_w]\{\tilde{B}\}^T \tag{9}$$

where $[Q_w]$ is the intensity matrix of the Gaussian white noise $\hat{w}$. The Hessenberg-Schur method[42] is used to solve Eq. (9).

Behavior Functions and Behavior Sensitivity Analysis

The following behavior functions can be evaluated with the present capability: elastic displacements, elastic twist, spar/rib cap stresses, skin combined stress failure criteria,[43] natural frequencies, real and imaginary parts of aeroservoelastic poles, rms of random control surface rotations and rotation rates due to gust, rms of sensor measurements in gust, total mass, lift and drag coefficients, control surface rotations and hinge moments in maneuvers, and roll rate or load factor in maneuvers. Control surface effectiveness is not addressed directly at this stage. Instead the synthesis focuses on sustaining a desired roll rate or load factor while keeping hinge moments, control surface deflections, and stresses within allowable bounds. Aeroservoelastic stability is guaranteed by providing sufficient damping at each flutter critical aeroservoelastic pole throughout the flight envelope.[44] Handling qualities can be addressed via inequality constraints on the aeroservoelastic pole locations (e.g., short period root placement) and pilot seat acceleration due to atmospheric turbulence.[45,46] The control surface rotation needed for trim and overall performance in a given maneuver and its rms activity due to gusts can be combined in a single constraint to avoid saturation.[47,48] Individual behavior functions or their combinations can serve as objective functions. Possible alternatives are mass, drag, rms of aileron rotation or rotation rate due to turbulence (to be minimized), steady roll rate or lift-to-drag ratio (to be maximized), or a combination of any of these.

Implicit differentiation of the analysis equations is used here to derive analytical expressions for the derivatives of all behavior functions with respect to all design variables.[24,49] This results in a computer code which is much larger and more complicated than one where finite difference derivatives are used. However, analytical sensitivities are free from numerical problems associated with finite difference step size selection and they are attractive in the context of multidisciplinary synthesis because of superior computational efficiency.

Approach to Integrated Optimization

Once the preassigned parameters, design variables, failure modes, load conditions, and objective function are selected, the integrated optimization problem can be cast as a nonlinear programming problem of the form

$$\min_{(\{X\})} F(\{X\}) \tag{10}$$

subject to

$$\{g\{X\}\} \le \{0\}$$

$$\{X\}^L \le \{X\} \le \{X\}^U$$

The nonlinear programming approach combined with approximation concepts (NLP/AC approach) has proven to be an effective method for solving structural synthesis problems[12,13] and here it is adapted to the multidisciplinary design optimization task. In this method relatively few detailed analyses are carried out during optimization. Each analysis and the associated behavior sensitivity analysis serve as a basis for constructing approximations to the objective and constraint functions in terms of the design variables. Thus, a series of explicit approximate optimization problems is solved converging to an optimal design. The main advantage of this approach is in its generality. No a priori assumptions have to be made about the set of active constraints at the optimum. Given an initial design, a local optimum is sought using mathematical programming techniques. Thus, it is especially suitable for multidisciplinary optimization, where the problem is large and complicated and past experience does not provide much intuitive guidance. However, for this approach to be practical it is crucial to avoid too many detailed analyses. Efficient analysis/sensitivity calculations and robust, explicit approximations are essential in this context. The CONMIN code[50] is used here for constrained function minimization. Reciprocal approximations were used for stress and aeroservoelastic pole location constraints. Hybrid approximations were used for gust-response rms values. For the minimum gauge constraints direct approximations were used. Since the gauge constraints are linear in the structural design variables [Eq. (3)], we have exact expresssions for these constraints.[49]

Test Case

The accuracy, power, and computational efficiency of the present capability are discussed in Ref. 24 using a mathematical model of a lightweight fighter similar to the YF-16. For the present optimization studies, a mathematical model of a small remotely piloted vehicle (RPV) is used. Its planform geometry is shown in Fig. 3. A biconvex 10% t/c wing is actively controlled by a small control surface located at about 80% semispan towards the tip. The control surface chord is 20% of the local wing chord, and it is driven by an actuator whose transfer function is preassigned

$$\frac{q_{c1}}{\delta_1} = \frac{1.7744728 \cdot 10^7}{(s+180)(s^2+251s+314^2)} \tag{11}$$

The wing control surfaces are only used for active flutter control. The elevators are used for rigid-body pitch and roll. The elevator actuator transfer function is

$$\frac{q_{c2}}{\delta_2} = \frac{20}{(s+20)} \tag{12}$$

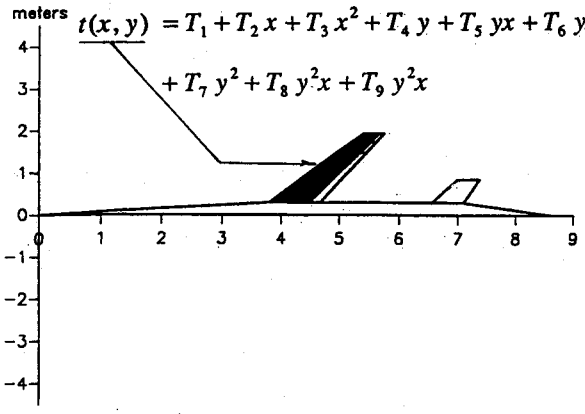

Fig. 3 Drone geometric layout.

q_{ci} and δ_i are the actual control surface rotation and actuator command, respectively. The RPV structure is modeled as an assembly of four equivalent plates. A flexible wing is attached to a rigid fuselage and rigid control surfaces. The wing is divided into three trapezoids. The two trailing-edge extensions, to the left and right of the control surface, are assumed fixed. The main wing box structure, extending from root to tip spanwise and to 80% chordwise, is the structure to be synthesized. The weight of fuselage, control surfaces, and nonstructural wing mass is 308 kg for a half-airplane. A Dryden gust model with a scale length of 518.16 m and a vertical gust rms velocity of 1.06 m/s is used. Following Refs. 51 and 52, an accelerometer is placed on the wing strip containing the control surface. It is located in the middle (spanwise) and 0.65 chord point of the strip. Its measurement serves as an input to a control law which, in turn, generates an input command δ to the actuator of the wing control surface. The set of three load conditions for wing stress calculations consists of 2-g symmetric pull-ups at sea level, 10,000, and 20,000 ft. In the "maneuver load" calculations [Eq. (5)] the airplane is trimmed using the elevator. All stress constraints reflect a 1.5 safety factor. Flutter, gust, and aeroservoelastic stability calculations, though, are carried out at sea level, Mach 0.9 for the cantilevered wing in the examples described herein. This is done intentionally in order to first examine flutter suppression/ structural optimization using a realistic but simple example, leaving flight mechanics issues for future studies.

It should be re-emphasized that the previous simplifying assumptions are made only for illustrative purposes and to facilitate physical interpretation of the design optimization results. The present capability can handle airplane models where multiple equivalent plate elements are synthesized subject to several pull-up or rolling maneuvers. Control systems can contain many control elements and control laws, and aeroservoelastic/gust response analyses can be carried out for symmetric/antisymmetric free-free motion in several flight conditions. The modeling detail and model size are only limited by available computer memory. The CPU time limits will determine the number of load conditions and flight conditions for aeroservoelastic/gust-response analysis. However, as shown later, quite complex problems can be handled with reasonable computer resources.

The control law used for this study is the localized damping type transfer function (LDTTF) described in Ref. 53. This low-order control law provides damping "locally" in the range of frequencies where damping is needed. Its form is

$$\delta = \frac{a_c}{s^2 + b_c s + c_c} y_{SE} \tag{13}$$

The denominator coefficients can be associated with equivalent damping ζ_c and natural frequency ω_c of the control law

$$c_c = \omega_c^2 \tag{14}$$

$$b_c = 2\zeta_c \omega_c \tag{15}$$

Thus, c_c and b_c determine the center frequency and gain peak width of the control law transfer function while a_c determines the effective gain. The preassigned accelerometer transfer function is

$$\frac{y_{SE}}{\ddot{w}_{0.65c}} = \frac{314^2}{s^2 + 376.8s + 314^2} \tag{16}$$

The LDTTF control law is used here without compensation for sensor and actuator transfer functions.[52]

Results

For a first sequence of numerical studies, a wing tip pod is added to the wing simulated by two 2.5 kg masses at the forward and aft points of the tip. The wing box construction consists of all aluminum cover skins and there are no spars or ribs in order to simplify the model and introduce as few structural design variables as possible. All stress carrying capacity is thus confined to the skins, which are held together mathematically by the plate assumptions and in practice by an array of minimum gauge spars/ribs whose stiffness can be neglected. The Von Mises yield criteria is used. The skin-thickness distribution is represented by a nine-term polynomial in x and y, whose terms are formed from the polynomial product $(1,x,x^2)(1,y,y^2)$. It then follows that the participation coefficients T_i [see Eq. (3)] serve as the nine structural design variables. Several alternative objective functions can be considered using the new design capability. In the following examples, however, the objective function to be minimized first is the wing box skin mass. Figure 4 shows skin-mass convergence histories for three synthesis cases, all starting with a 1 mm (0.0393 in.) uniform skin-thickness distribution. In the first case, mass is minimized subject to stress and minimum gauge constraints only. Minimum skin thickness is taken to be 0.381 mm (0.015 in.), and the Von Mises equivalent stress and minimum gauge are constrained at 25 points over the wing box surface (5 chordwise × 5 spanwise). This is the "stress design" without flutter constraints. In this case, the skin mass is reduced in 11 full analyses/approximate problem optimization cycles from 4.486 to 1.743 kg.

The stress design is aeroelastically unstable. It flutters at sea level, Mach 0.9, and thus, a second synthesis is carried out. The same nine structural design variables are used and the same stress and minimum gauge limitations are imposed; however, dynamic aeroelastic stability constraints are now added to the set of requirements that must be satisfied. It is required that at sea level, Mach 0.9, there should be at least 4.5% equivalent viscous damping in the two lowest frequency poles,

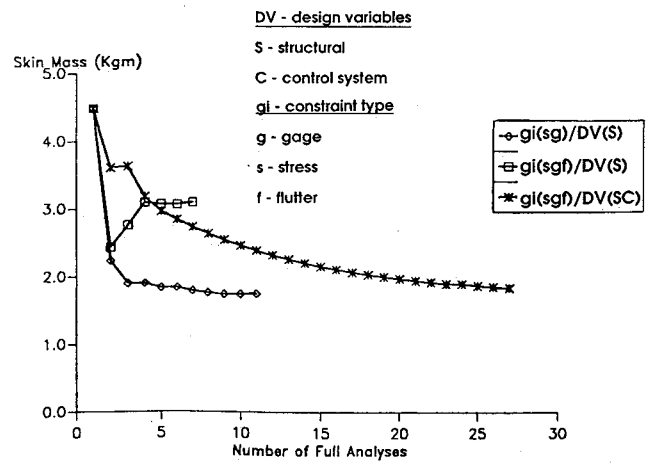

Fig. 4 Skin-mass iteration histories with different constraints and design variables.

and at least 1.5% damping in the next three (aerodynamic poles which have very large damping ratios are ignored when the closed-loop system poles are ordered by damped frequency). In seven synthesis cycles, the optimization process generates a design with a skin mass of 3.094 kg. This is the "flutter design." As expected, a stiffer and heavier wing is needed to prevent flutter. The constraint which drives this design is a damping constraint associated with a flutter pole at 14.4 Hz.

An important question is addressed next: If we are unwilling to pay in terms of structural weight, how effective can an active control system be in further reducing the minimum structural weight needed to satisfy stress and flutter constraints? Three control system design variables are now added to the nine structural design variables. Wing skin-mass minimization is carried out (control system mass is not taken into account at this stage) subject to stress, minimum gauge, and dynamic aeroelastic stability constraints starting from a 1-mm-thick uniform skin and a control law:

$$\frac{\delta}{y_{SE}} = \frac{2000}{s^2+40s+10{,}000} \tag{17}$$

As shown in Fig. 4, the skin mass for this case is reduced to 1.838 kg. Examination of the optimization results reveals that the driving constraint is again the damping at a pole. Its frequency is 17.03 Hz, and the final damping ratio is 0.067, which implies that with tighter convergence criteria for terminating the optimization, additional weight savings could be achieved (1% diminishing return on three consecutive approximate problem optimizations is used as a convergence criterion). In any event, the weight in the third case (1.838 kg) is brought back almost to the level of the stress design weight (1.743 kg) although convergence is slower. The third case required 27 cycles and 27 CPU min on the University of California at Los Angeles IBM 3090-4 to converge. Also, whereas rapid convergence was achieved for the cases with only structural design variables using 40% move limits, it was necessary to use 10% move limits when control system design variables were added (in order to protect the accuracy of system pole approximations). This explains the slower convergence in the third case.

Minimum mass synthesis of the wing with structural and control system design variables, subject to stress, gauge, and aeroservoelastic stability constraints was tried again. This time the initial structural design is the unstable stress design found at the end of 11 iterations in the first case. Different initial values for control system design variables are used. The optimization is started with

$$\frac{\delta}{y_{SE}} = \frac{1500}{s^2+40s+4000} \tag{18}$$

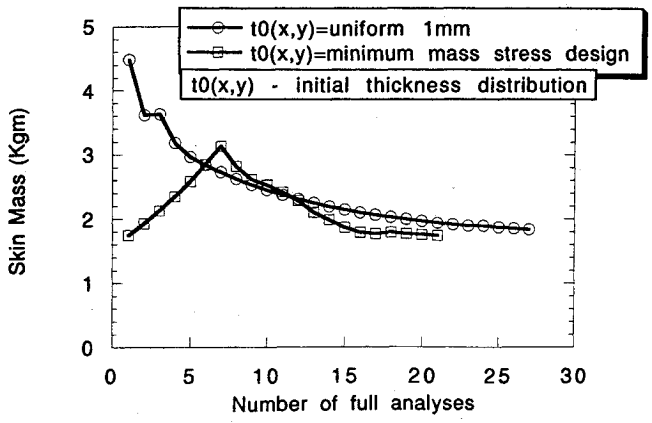

Fig. 5 Control/structure synthesis skin-mass convergence histories (different initial designs).

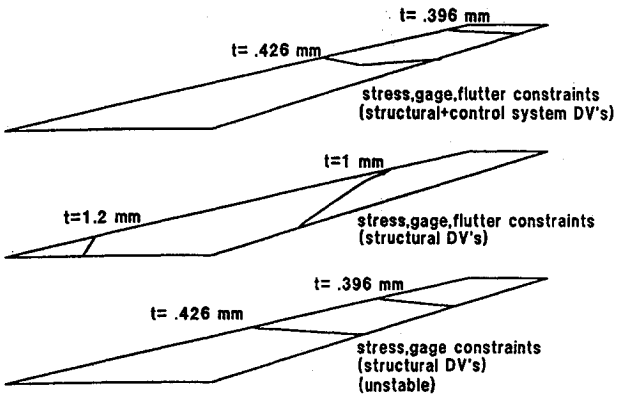

Fig. 6 Minimum weight aluminum skin-thickness distributions.

Figure 5 shows the two skin-mass convergence histories: one for the design starting from 1-mm uniform skin and the other starting from the stress design. Starting with the 1.743 kg skin of the stress design, the mass minimization progresses by first adding mass to stiffen the wing followed by manipulation of the control system design variables to stabilize the wing with the smallest weight penalty possible. In fact, the final skin weighs 1.745 kg, essentially the same as if there were no flutter constraints at all (i.e., 1.743 kg). Final skin-thickness distributions for the stress, stress plus flutter, and stress plus actively controlled flutter designs are shown in Fig. 6. The penalty in weight, when only structural design variables are used and the flutter constraint is imposed, is clearly associated with a required increase in wing torsional stiffness. The final control laws for the two cases shown in Fig. 5 are $1517.7/(s^2+51.4s+15{,}072.9)$ and $1456.7/(s^2+40.2s+15{,}310.4)$ for the 1-mm initial design and stress initial design, respectively. It is interesting to note that the numerator terms (effective gains) converge from different starting points to values that are within 5% from each other. The constant denominator terms in both final control laws are almost the same indicating that active damping is introduced at a band of frequencies around 19.6 Hz. This result is intuitively rewarding since the flutter mechanism seems to involve a wing bending root at 16–17 Hz and a second root at 25–26 Hz. The control law's localized damping action is thus tuned so as to be approximately in the middle of this band. The width of the frequency band is controlled by the equivalent control law damping parameter ζ_c which is 21% and 16% for the two cases in Fig. 5. The results described so far indicate that, as long as controllability and observability are guaranteed, an active control system of unlimited power based on aerodynamic energy concepts[51–53] can stabilize the wing and avoid essentially all structural weight penalty that would have been needed to achieve this in a passive manner. Even when gust dynamic stresses become critical in the stress design (in addition to the quasistatic stresses included here), it is reasonable to believe that a powerful control system can save a substantial amount of structural weight.

The next objective is to study how limits on the power of the control system effect an integrated design and how structural weight and control effort interact in the course of integrated optimization. If we are not willing to allocate any additional weight beyond the weight needed for strength, a control system can be designed for the stress design so as to take care of its instability. It is desirable, of course, to require that such a control system will consume as little power as possible. The rms values of control surface rotation q_c and rotation rate $\dot{q}_c$ serve as measures of control system effort and limitations.[3,51,52] The synthesis problem for this case is formulated as follows: Freeze the structural stress design. Allow changes in the three control system design variables only. Minimize the rms value of the aileron rotation due to gusts subject to the same stability constraints as in the previous design studies. This is a control system optimization problem in which the

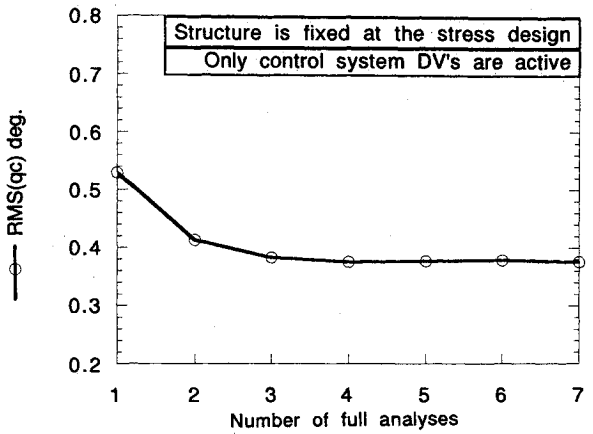

Fig. 7 Minimization of aileron rms rotation due to turbulence (control system—variable, structural "stress design"—fixed).

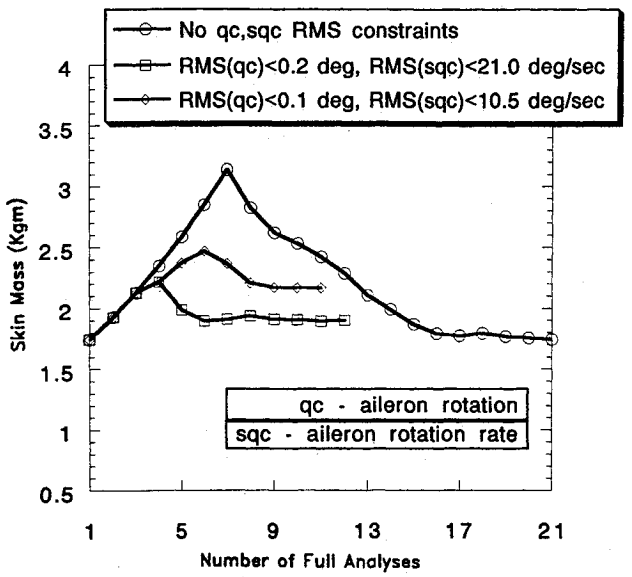

Fig. 8 Convergence histories for control/structure skin-mass minimizations with gauge, stress, flutter, and gust-response constraints.

"best" control law of given order is sought to minimize aileron gust response and guarantee stability of a given aeroelastic plant. Figure 7 shows a history of aileron rms rotation during optimization. The optimization converges to a control system design of the form: $1699.6/(s^2+21.58s+15{,}853.6)$. The minimum rms rotation is 0.374 deg and the associated rms of rotation rate is 40 deg/s. Move limits of 10% were used.

Returning to skin-mass minimization, gust-response constraints are now added to the previous set of constraints. In two cases these rms values were constrained placing limitations of varying severity on the control system. Figure 8 depicts three mass convergence iteration histories all starting with the stress design: 1) no bounds on the rms q_c and $\dot{q}_c$; 2) rms $q_c \leq 0.2$ deg, rms $\dot{q}_c \leq 21.0$ deg/s; 3) rms $q_c \leq 0.1$ deg, rms $\dot{q}_c \leq 10.5$ deg/s. Move limits of 10% were used for all three cases. Nine structural and three control system design variables are used simultaneously. As Fig. 8 shows, convergence within 12 optimization cycles is achieved when the gust-response constraints are added to the stress, gauge, and stability constraints. When control surface activity is more restricted, the final skin weight is larger. Thus, limited control system resources are traded off against structural resources in a quest for a balanced multidisciplinary optimum design. This interaction takes place dynamically as the synthesis progresses and it is hard or impossible to capture in sequential parametric studies.

Of course, it might be argued that control system power translates in the end to added mass, and that for the tradeoff studies to be more realistic, we need to include the weight of the control system in the objective function. The current capability can take this into account by linking the values of certain concentrated masses to the rms aileron rotation and rotation rate needed. This capability was not used, however, in the examples given here.

Figure 9 adds to the understanding of interdisciplinary interactions by showing the evolution of skin mass (normalized with respect to the stress design mass), an active stability constraint, and an active gust-response constraint in the course of optimization for the third case in Fig. 8. Constraints are posed as $g_i \leq 0.0$. Thus, when a constraint is violated it is positive, and when it is active in the final design it is within a small neighborhood of zero. As shown, the wing is unstable at the initial design point (stability constraint violated) and the first

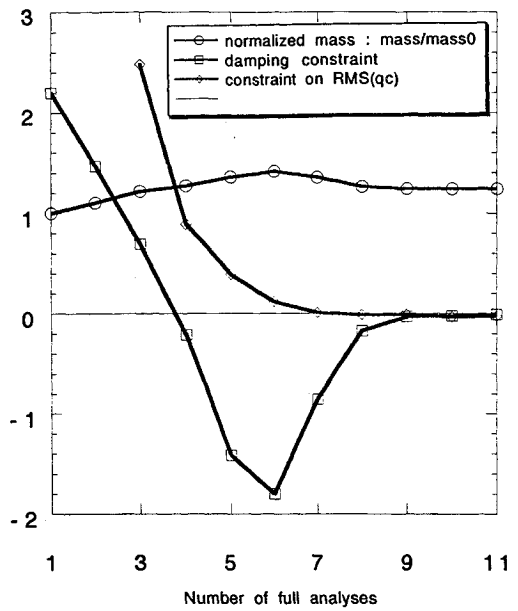

Fig. 9 Behavior function evolution during the minimum mass skin synthesis with stress, flutter, and gust-response constraints.

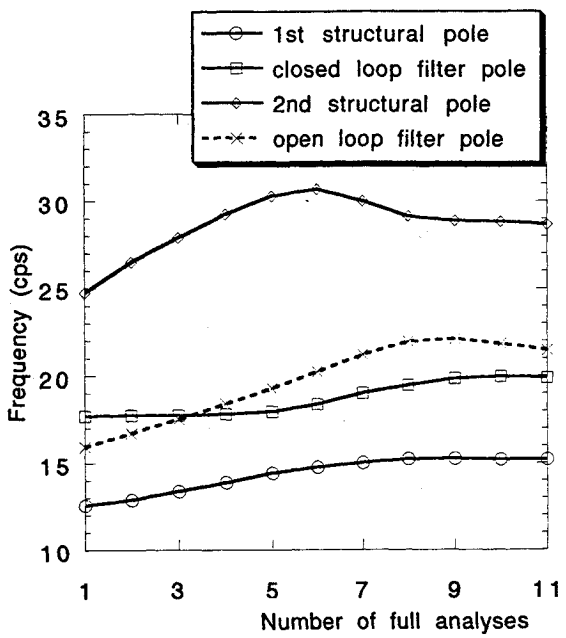

Fig. 10 Evolution of closed-loop damped frequencies during aeroservoelastic wing/control system design.

several optimization cycles produce designs that are more stable than needed (stability constraint strictly less than zero). The synthesis then progresses by driving the gust-response constraint to the feasible region and at the same time reducing stability to the minimum allowed value of damping (bringing the stability constraint back to zero) so as to gain further reduction in structural weight. No gust-response calculations are carried out as long as the system is unstable and the synthesis focuses on stabilizing the wing by varying the structural and control system design variables simultaneously. For stable designs along the synthesis path, gust-response calculations are carried out. Using 10% move limits, hybrid approximations are apparently adequate for the gust and aeroservoelastic pole constraint approximations in this example. Following the evolution of a physically significant control system variable, namely, the equivalent natural frequency of the control law transfer function ω_c [see Eqs. (14) and (15)], Fig. 10 shows how this frequency moves to center itself between the two lowest frequency structural poles so as to introduce damping into both.

Concluding Remarks

A new capability for integrated, control augmented, structural synthesis of practical wings has been used for exploratory studies focusing on structure/active-control interaction in a simple RPV wing. The results presented here do not reflect the full capacity and power of this new capability (many more examples illustrating multidisciplinary optimization of wings can be found in Ref. 54). However, the results presented here serve to demonstrate successful adaptation of NLP/AC techniques to problems with important new types of constraints (aeroservoelastic stability, gust response) exhibiting greater complexity than those previously treated in pure structural synthesis problems or in integrated design optimization studies based on simplified models. The importance of integration in multidisciplinary synthesis is demonstrated, as limited resources in different disciplines compete dynamically and interactively throughout the design process in the search for an improved design. Further numerical studies, involving more disciplines, richer blends of constraints and design variables, and more complicated configurations are planned for the near future.

Acknowledgment

This research was supported by Air Force Office of Scientific Research Contract F49620-87-K-0003.

References

[1]Hwang, C., and Kesler, D. F., "Aircraft Active Controls—New Era in Design," *Astronautics & Aeronautics,* June 1983, pp. 70–85.

[2]Hanson, P. W., "An Aeroelastician's Perspective of Wind Tunnel and Flight Experiences with Active Control of Structural Response and Stability," NASA TM-85761, April 1984 (available from NTIS as N84-23924).

[3]Newsom, J. R., Adams, W. M., Mukhopadhyay, V., Tiffany, S. H., and Abel, I., "Active Controls: A Look at Analytical Methods and Associated Tools," International Council of Aeronautical Sciences, *Proceedings of the 14th Congress of the International Council of the Aeronautical Sciences,* AIAA, New York; ICAS Paper ICAS-84-4.2.3, 1984.

[4]McCullers, L. A., "Automated Design of Advanced Composite Structures," *Mechanics of Composite Materials,* edited by Zvi Hashin, Pergamon, Oxford, England, UK, 1983, pp. 119–133.

[5]Shirk, M. H., Hertz, T. J., and Weisshaar, T. A., "Aeroelastic Tailoring—Theory, Practice, Promise," *Journal of Aircraft,* Vol. 23, No. 1, 1986, pp. 6–18.

[6]Weisshaar, T. A., "Aeroelastic Tailoring—Creative Uses of Unusual Materials," *Proceedings of the AIAA/ASME/ASCE/AHS 28th Structures, Structural Dynamics, and Materials Conference,* AIAA, New York, 1987; also AIAA Paper 87-0976, April 1987.

[7]Felt, L. R., Huttsell, L. J., Noll, T. E., and Cooley, D. E., "Aeroservoelastic Encounters," *Journal of Aircraft,* Vol. 16 No. 7, 1979, pp. 477–483.

[8]Freyman, R., "Interactions Between an Aircraft Structure and Active Control Systems," *Journal of Guidance, Control, and Dynamics,* Vol. 10, No. 5, 1987, pp. 447–452.

[9]Tolson, R. H., and Sobieszczanski-Sobieski, J., "Multidisciplinary Analysis and Synthesis: Needs and Opportunities," *Proceedings of the AIAA/ASME/ASCE/AHS 26th Structures, Structural Dynamics, and Materials Conference,* AIAA, New York; AIAA Paper 85-0584, 1985.

[10]Sobieszczanski-Sobieski, J., and Haftka, R. T., "Interdisciplinary and Multilevel Optimum Design," *Computer Aided Optimal Design: Structural and Mechanical Systems,* edited by C. A. Mota Soares, Springer-Verlag, Berlin, 1987, pp. 655–701.

[11]Weisshaar, T. A., Newsom, J. R., Zeiler, T. A., and Gilbert, M. G., "Integrated Structure/Control Design—Present Methodology and Future Opportunities," International Council of Aeronautical Sciences, ICAS Paper ICAS-86-4.8.1, 1986 Conf. of the International Council of the Aeronautical Sciences, London, England.

[12]Schmit, L. A., "Structural Analysis—Precursor and Catalyst," *Recent Experiences in Multidisciplinary Analysis and Optimization,* NASA CP-2327, Pt. 1, April 1984, pp. 1–17.

[13]Schmit, L. A., "Structural Optimization—Some Key Ideas and Insights," *New Directions in Optimum Structural Design,* edited by E. Atrek, R. H. Gallagher, K. M. Ragsdell, and O. C. Zienkiewicz, Wiley, New York, 1984, pp. 1–35.

[14]Lynch, R. W., and Rogers, W. A., "Aeroelastic Tailoring of Composite Materials to Improve Performance," *Proceedings of the 16th AIAA Structures, Structural Dynamics, and Materials Conference,* AIAA, New York, 1975, pp. 61–68.

[15]Haftka, R. T., "Optimization of Flexible Wing Structures Subject to Strength and Induced Drag Constraints," *AIAA Journal,* Vol. 15, No. 8, 1977, pp. 1101–1106.

[16]Wilkinson, K., Markowitz, J., Lerner, E., George, D., and Batill, S. M., "FASTOP—A Flutter and Strength Optimization Program for Lifting Surface Structures," *Journal of Aircraft,* Vol. 14, No. 6, 1977, pp. 581–587.

[17]Lecina, G., and Petiau, C., "Advances in Optimal Design with Composite Materials," *Computer Aided Optimal Design: Structural and Mechanical Systems,* edited by C. A. Mota Soares, Springer-Verlag, Berlin, 1987, pp. 943–953.

[18]Neill, D. J, Johnson, E. H. and Canfield, R., "ASTROS—A Multidisciplinary Automated Structural Design Tool," *Proceedings of the AIAA/ASME/ASCE/AHS 28th Structures, Structural Dynamics, and Materials Conference,* AIAA, New York, 1987; also AIAA Paper 87-0713.

[19]Grossman, B., Gurdal, Z., Strauch, G. J., Eppard, W. M., and Haftka, R. T., "Integrated Aerodynamic/Structural Design of a Sailplane Wing," *Journal of Aircraft,* Vol. 25, No. 9, 1988, pp. 855–860.

[20]Wrenn, G. A., and Dovi, A. R., "Multilevel Decomposition Approach to the Preliminary Sizing of a Transport Wing," *Journal of Aircraft,* Vol. 25, No. 7, 1988, pp. 632–638.

[21]Zeiler, T. A., and Weisshaar, T. A., "Integrated Aeroservoelasic Tailoring of Lifting Surfaces," *Journal of Aircraft,* Vol. 25, No. 1, 1988, pp. 76–83.

[22]Morris, S., and Kroo, I., "Aircraft Design Optimization with Multidisciplinary Performance Criteria," *Proceedings of the AIAA/ASME/ASCE/AHS/ASC 30th Structures, Structural Dynamics, and Materials Conference,* AIAA, Washington, DC; AIAA Paper 89-1265, 1989.

[23]Dracopoulos, T. N., and Oz, H., "Integrated Aeroelastic Control Optimization," 7th VPI&SU/AIAA Symposium on Dynamics and Control of Large Structures, VA, May 1989.

[24]Livne, E., Schmit, L. A., and Friedmann, P. P., "Towards an Integrated Approach to the Optimum Design of Actively Controlled Composite Wings," *Journal of Aircraft,* Vol. 27, No. 12, 1990, pp. 979–992.

[25]Livne, E., Schmit, L. A., and Friedmann, P., "Design Oriented Structural Analysis for Fiber Composite Wings," Univ. of California, UCLA-ENG-88-36, Los Angeles, CA, Nov., 1988.

[26]Giles, G. L., "Equivalent Plate Analysis of Aircraft Wing Box Structures with General Planform Geometry," *Journal of Aircraft,* Vol. 23, No. 11, 1986, pp. 859–864.

[27]Lottati, I., and Nissim, E., "Three-Dimensional Oscillatory Piecewise Continuous Kernel Function Method," in three parts, *Journal of Aircraft,* Vol. 18, No. 5, 1981, pp. 346–363.

[28]Lottati, I., and Nissim, E., "Nonplanar, Subsonic, Three Dimensional Oscillatory Piecewise Continuous Kernel Function Method," *Journal of Aircraft,* Vol. 22, No. 12, 1985, pp. 1043–1048.

[29]Nissim, E., and Lottati, I., "Supersonic Three-Dimensional Oscillatory Piecewise Continuous Kernel Function Method," *Journal of Aircraft,* Vol. 20, No. 8, 1983, pp. 674–681.

[30]Lottati, I., "Induced Drag and Lift of Wing by the Piecewise Continuous Kernel Function Method," *Journal of Aircraft,* Vol. 21, No. 11, 1984, pp. 833–834.

[31]Roger, K. L., "Airplane Math Modeling Methods for Active Control Design," *Structural Aspects of Active Controls,* AGARD CP-228, Aug. 1977, pp. 4–11.

[32]Karpel, M., "Design for Active Flutter Suppression and Gust Alleviation Using State Space Aeroelastic Modeling," *Journal of Aircraft,* Vol. 19, No. 3, 1982, pp. 221–227.

[33]Tiffany, S. H., and Adams, W. M., "Nonlinear Programming Extensions to Rational Function Approximations of Unsteady Aerodynamics," *Proceedings of the AIAA/ASME/ASCE/AHS/ASC 28th Structures, Structural Dynamics, and Materials Conference,* AIAA, New York, 1987, pp. 406–420; also AIAA Paper 87-0854.

[34]Rowe, W. S., "Comparison of Analysis Methods Used in Lifting Surface Theory," *Computational Methods in Potential Aerodynamics,* edited by L. Morino, Springer-Verlag, Berlin, 1985, pp. 197–240.

[35]Schmidt, W., "Advanced Numerical Methods for Analysis and Design in Aircraft Aerodynamics," *International Journal of Vehicle Design,* Vol. 7, No. 3/4, 1986, pp. 415–440.

[36]Rogers, W. A., Brayman, W. W., and Shirk, M.H., "Design, Analysis, and Model Tests of an Aeroelastically Tailored Lifting Surface," *Journal of Aircraft,* Vol. 20, No. 3, 1983, pp. 208–215.

[37]Rodden, W. P., and Giesing, J. P., "Application of Oscillatory Aerodynamic Theory to Estimation of Dynamic Stability Derivatives," *Journal of Aircraft,* Vol. 7, No. 3, 1970, pp. 272–275, (Errata and Addenda in *Journal of Aircraft,* Vol. 21, No. 1, 1984, pp. 93–94).

[38]Haftka, R. T., and Yates, E. C., Jr., "Repetitive Flutter Calculations in Structural Design," *Journal of Aircraft,* Vol. 13, No. 7, 1976, pp. 454–461.

[39]Livne, E., "Accurate Calculation of Control-Augmented Structural Eigenvalue Sensitivities Using Reduced Order Models," *AIAA Journal,* Vol. 27, No. 7, 1989, pp. 947–954.

[40]Karpel, M., "Efficient Vibration Mode Analysis of Aircraft with Multiple External Store Configurations," *Journal of Aircraft,* Vol. 25, No. 8, 1988, pp. 747–751.

[41]Bryson, A. E., and Ho, Y. C., *Applied Optimal Control,* Hemisphere, Washington, DC, Revised Printing, 1975, Chap. 11.

[42]Golub, G. H., Nash, S., and Van Loan, C., "A Hessenberg-Schur Method for the Problem $AX+XB=C$," *IEEE Transactions on Automatic Control,* Vol. AC-24, No. 6, 1979, pp. 909–913.

[43]Tsai, S. W., and Hahn, H. T., *Introduction to Composite Materials,* Technomic Publishing, Westport, CT, 1980, Chap. 7.

[44]Hajela, P., "A Root Locus-Based Flutter Synthesis Procedure," *Journal of Aircraft,* Vol. 20, No. 12, 1983, pp. 1021–1027.

[45]Rimer, M., Chipman, R., and Muniz, B., "Control of a Forward Swept Wing Configuration Dominated by Flight Dynamics/Aeroelastic Interactions," *Journal of Guidance, Control, and Dynamics,* Vol. 9, No. 1, 1986, pp. 72–79.

[46]Moynes, J. F., and Gallagher, J. T., "Flight Control System Design for Ride Qualities of Highly Maneuverable Fighter Aircraft," *Guidance and Control Design Considerations for Low Altitude and Terminal Area Flight,* AGARD CP-240, April 1978.

[47]Beaufrere, H., "Limitations of Statically Unstable Aircraft due to the Effects of Sensor Noise, Turbulence, and Structural Dynamics," *Proceedings of the AIAA Guidance, Navigation, and Control Conference;* AIAA Paper 86-2203, Aug. 1986.

[48]Yamamoto, T., "Impact of Aircraft Structural Dynamics on Integrated Control Design," *Proceedings of the AIAA Guidance, Navigation, and Control Conference;* AIAA Paper 83-2216, Aug. 1983.

[49]Haftka, R. T., and Kamat, M. P., *Elements of Structural Optimization,* Martinus Nijhoff, Dordrecht, The Netherlands, 1985, Chap. 6.

[50]Vanderplaats, G. N., *Numerical Optimization Techniques for Engineering Design: With Applications,* McGraw-Hill, New York, 1984.

[51]Nissim, E., and Abel, I., "Development and Application of an Optimization Procedure for Flutter Suppression Using the Aerodynamic Energy Concept," NASA TP-1137, Feb. 1978.

[52]Nissim, E., "Design of Control Laws for Flutter Suppression Based on the Aerodynamic Energy Concept and Comparisons with Other Design Methods," *Proceedings of the AIAA/ASME/ASCE/AHS/ASC 30th Structures, Structural Dynamics, and Materials Conference;* AIAA Paper 89-1212, April 1989.

[53]Nissim, E., "Recent Advances in Aerodynamic Energy Concept for Flutter Suppression and Gust Alleviation using Active Controls," NASA TN D-8519, Sept. 1977.

[54]Livne, E., "Integrated, Multidisciplinary Optimization of Actively Controlled, Fiber Composite Wings," Ph.D. Dissertation, Mechanical, Aerospace and Nuclear Engineering Dept., University of California, Los Angeles, Los Angeles, CA, Sept. 1990.